Biochimica et Biophysica Acta 1814 (2011) 1862–1869

Contents lists available at ScienceDirect

Biochimica et Biophysica Acta

journal homepage: www.elsevier.com/locate/bbapap

A novel approach for the characterisation of proteoglycans and biosynthetic enzymes in a snail model ☆

Tarsis F. Gesteira [a,1], Vivien Jane Coulson-Thomas [a,1], Fernando T. Ogata [a,1], Eduardo H.C. Farias [a,1], Renan P. Cavalheiro [a,1], Marcelo A. de Lima [a,1], Gabriel L.A. Cunha [a,1], Ernesto S. Nakayasu [b,2], Igor C. Almeida [b], Leny Toma [a,1], Helena B. Nader [a,*]

[a] Departamento de Bioquímica, Universidade Federal de São Paulo, Rua Três de Maio, 100, 04044-020 São Paulo, SP, Brazil
[b] The Border Biomedical Research Center, Department of Biological Sciences, University of Texas at El Paso, El Paso, TX 79912, USA

ARTICLE INFO

Article history:
Received 21 March 2011
Received in revised form 13 July 2011
Accepted 29 July 2011
Available online 5 August 2011

Keywords:
Achatina fulica
Glycosaminoglycan
Acharan sulfate
Immunohistochemistry
Proteomic analysis

ABSTRACT

Proteoglycans encompass a heterogeneous group of glycoconjugates where proteins are substituted with linear, highly negatively charged glycosaminoglycan chains. Sulphated glycosaminoglycans are ubiquitous to the animal kingdom of the Eukarya domain. Information on the distribution and characterisation of proteoglycans in invertebrate tissues is limited and restricted to a few species. By the use of multidimensional protein identification technology and immunohistochemistry, this study shows for the first time the presence and tissue localisation of different proteoglycans, such as perlecan, aggrecan, and heparan sulphate proteoglycan, amongst others, in organs of the gastropoda *Achatina fulica*. Through a proteomic analysis of Golgi proteins and immunohistochemistry of tissue sections, we detected the machinery involved in glycosaminoglycan biosynthesis, related to polymer formation (polymerases), as well as secondary modifications (sulphation and uronic acid epimerization). Therefore, this work not only identifies both the proteoglycan core proteins and glycosaminoglycan biosynthetic enzymes in invertebrates but also provides a novel method for the study of glycosaminoglycan and proteoglycan evolution.

1. Introduction

The complex structure and heterogeneity of the glycosaminoglycan (GAG) chain play an important role in the myriad of biological functions attributed to proteoglycans. The proteoglycan biosynthesis starts in the late endoplasmatic reticulum and/or the cis-Golgi compartment [1–6], with the xylosylation of specific serine residues on the core protein [7–10]. The following step is the chain elongation by the action of glycosyltransferases that successively transfer hexosamine and hexuronic acid. Distinct modifications at specific sites along the chain then occur in the medial- and trans-Golgi compartments. For heparan sulphate (HS) and heparin (HEP), specific modifications by different types of enzymes occur: N-deacetylase-N-sulphotransferase, glucuronosyl C-5 epimerase, 2,3 and 6-O sulphotransferases, thereby providing the enormous diversity of GAG chains which are required for the different biological functions [11–15,65]. The heterogeneity of the GAG chain is further regulated according to the cell cycle and cell–cell contact, enabling interactions with different surface proteins and effectors. The study of this complex biosynthetic machinery, responsible for the synthesis of distinct GAG chains, is challenging and requires novel analytical techniques for precise characterisation.

GAGs are distributed throughout the animal kingdom in both vertebrate and invertebrate phylogenetic tree [16–19]. Acharan sulphate (AS) is a GAG primarily isolated from the giant African snail (*Achatina fulica*) composed of α-D-N-acetylglucosaminyl-2-O-sulpho-α-L-iduronic acid repeating units, which relates to the structure of HEP and HS; however, AS shows important differences to these GAGs [20–22]. For instance, the glucosamine residue bearing N-acetyl substitution in the AS chain contradicts the current GAG biosynthetic pathway theory, where N-sulphation and epimerization precede 2-O-sulphation. Hence, *A. fulica* is an interesting model for studying GAG biosynthesis [23,24].

Proteoglycans encompass a heterogeneous group of glycoconjugates where proteins are substituted with linear, highly negatively charged GAG chains. Due to the presence of carboxyl and sulphate groups, GAGs constitute a major source of macromolecular polyanions that surround almost every cell type in metazoan organisms. Except for hyaluronic acid, all GAGs occur in the tissues as proteoglycans [13,18,25,26]. GAGs can be differentiated regarding the type of hexosamine and non-nitrogenated sugar moieties, degree and position of sulphation, as well

☆ This work is dedicated to the memory of Professor Carl Peter von Dietrich.

* Corresponding author at: Departamento de Bioquímica, Universidade Federal de São Paulo, Rua Três de Maio, 100, 04044-020 São Paulo, SP, Brazil. Tel.: +55 11 55793175; fax: +55 11 5573 6407.
E-mail address: hbnader.bioq@epm.br (H.B. Nader).
[1] Fax: +55 11 5573 6407.
[2] Present address: Pacific Northwest National Laboratory, Richland, WA 99352, USA.

1570-9639
doi:10.1016/j.bbapap.2011.07.024

as the type of inter- and intradisaccharide glycosydic linkages. Sulphated GAGs are ubiquitous to the animal kingdom of the Eukarya domain, whereas in the bacteria kingdom only non-sulphated chains of GAGs are found. Sulphated GAGs are absent in protista, plantae, and fungi. In the animal kingdom, the appearance of HS and CS coincides with the emergence of eumetazoa, which are animals that display true tissues. These compounds are ubiquitously found in all tissues and species analysed. The occurrence of DS is a late event in the evolutionary GAG tree, being restricted to the appearance of deuterostomes. On the other hand, the distribution of HEP is scattered throughout the evolutionary tree, being found in some invertebrate and vertebrate species [13,18,27–29]. Studies reporting diverse and novel glycan structures have been described in invertebrates such as glucose branches in chondroitin sulphate from squid cartilage, heparin-like compounds in crab, and bivalve tissues and AS in *A. fulica* [4,27,30–34]. A number of biological functions have been proposed for AS in the snail such as an antidesiccant and antibiotic molecule for protection of the animal, as well as a role in locomotion and mobility, osmoregulation, transport of divalent cations, and reproduction [35]. Moreover, AS can act as an anti-angiogenic and tumour growth suppressor in cell and animal models [14,15,36,37]. Interestingly, AS is not present in *A. fulica* eggs; however, its content remarkably increases after hatching, suggesting an important role in the snail growth but not in the initial phases of development [38].The presence of proteoglycans in this snail has not been described to date. Thus, in the present paper a proteomic-based approach was used to study proteoglycans purified from the whole body of the snail and results were confirmed through immunohistochemistry of key organs. Moreover, this proteomic approach was also applied to a Golgi fraction purified from the whole snail in an attempt to describe putative enzymes involved in GAG synthesis, and the results were confirmed through immunohistochemistry utilising antibodies that recognise these enzymes. The results revealed for the first time the presence and localisation of different types of proteoglycans in *A. fulica*, as well as the description and localisation of GAG biosynthetic machinery in organs of the snail.

2. Material and methods

2.1. Snail extracts

Animals were collected from the city of Santos (São Paulo, Brazil) and processed after shell removal. The Animal Ethics Committee of the University according to Brazilian animal care legislation approved all experiments. For the proteoglycan extraction, the animals were rinsed in cold phosphate buffered saline (67 mM phosphate and 150 mM NaCl, pH 7.0), soft body (mollusc without the shell content) sliced with surgical blades on a glass plate and minced with 8 ml of buffer A (50 mM Tris, pH 7.4, containing 7 M urea, 0.1 M NaCl, 1 μg/ml aprotinine, 1 μg/ml leupeptine, 1 mM PMSF, 10 mM α-aminocaproic acid, 1 mM EDTA, 1 mM benzamidine, 5 mM iodoacetamide, and 5 mM DTT) for 48 h at 4 °C. Afterwards, the samples were centrifuged (3000 ×*g*, 5 min, 4 °C) in order to remove larger fragments. Aliquots (0.1 ml) of the supernatant were used for total protein determination, using the Bradford Reagent (Fermentas, Burlington, CA). For the stacked Golgi isolation, the whole body of *A. fulica* was finely dissected and minced using surgical blades on a glass Petri dish, placed into a 50-ml conical tube on ice and suspended at a ratio of 1 g of minced wet tissue per 2 ml of 0.5 M sucrose homogenization buffer (0.5 M sucrose, 5 mM $MgCl_2$, 0.1 M KH_2PO_4/K_2HPO_4 buffer, pH 6.7, and complete protease inhibitor mixture 250 μl/50 ml) (Roche Applied Science, Pleasanton, CA). The pieces were further homogenised using a Polytron homogeniser PT 10–35 (Brinkmann Instruments, Westbury, NY) for four cycles of less than 30 s and subjected to centrifugation (1500 ×*g* for 10 min at 4 °C). The supernatant was collected on ice and subjected to stacked Golgi isolation.

2.2. Proteoglycan purification and analysis

Proteoglycans were purified using Macro-Prep Q Support strong anion exchange resin (Bio-Rad, Hercules, CA) as described [39]. Briefly, the supernatant obtained as described above was added to the resin (5 ml supernatant/100 μl resin), incubated at 4 °C under rocking for 20 min and sedimented by centrifugation for 5 min at 3000 ×*g*. The resin was then washed for 5 min with the following buffers: one wash with buffer A (50 mM Tris, pH 7.4, containing 7 M urea, 0.1 M NaCl, complete protease inhibitor mixture (Roche Applied Science), and 5 mM DTT), two washes with buffer B (buffer A plus 0.1 M NaCl), three washes with buffer C (6 M urea, 0.2 M NaCl, and 50 mM sodium acetate, pH 3.7) and finally two washes with buffer B. The proteoglycans were eluted with 300 μl of 50 mM Tris, pH 7.4, 6 M urea and 1 M NaCl, subjected to SDS-PAGE electrophoresis using a mini protein system (Bio-Rad) and silver staining [40]. Proteoglycans were excised from the gel, subjected to tryptic in-gel digestion [41] or proteinase K (Invitrogen, Carlsbad, CA) in gel digestion [42] and the peptides extracted and separated using capillary columns (75-μm internal diameter by 10-cm length) packed with 10 mg/ml POROS C18 resin (10-μm particle size) (Applied Biosystems, Foster City, CA) in 100% acetonitrile with a high pressure apparatus at 500 psi [43]. The quality of packing was monitored in a stereomicroscope. Tryptic digested proteoglycan samples were suspended in 10 μl 20% 2-propanol/0.2% formic acid and loaded onto the capillary column connected to a nano-HPLC system (1D-Plus) (Eksigent, Dublin, CA). The samples were eluted (200 nl/min) in a gradient of 20–80% solvent B over 60 min (solvent A: 5% 2-propanol/0.2% formic acid; solvent B: 90% 2-propanol/0.2% formic acid) directly analysed in the nanospray source of a linear ion-trap mass spectrometer (LXQ, Thermo Fisher Scientific, Waltham, MA) as described in Section 2.5. A portion of the tryptic digested peptides/glycopeptides was also submitted to β-elimination followed by Michael addition with DTT [44]. Glycopeptides were incubated for 3 h at 50 °C in 20% ethanol, 10 mM DTT containing 0.1% NaOH and 1% triethylamine. The reaction was quenched by addition of 1% trifluoroacetic acid final concentration and the peptides extracted with packaged POROS R1-10 resin by elution with 70% acetonitrile in 0.1% trifluoroacetic acid.

2.3. Stacked Golgi isolation

The supernatant aliquots prepared from *A. fulica* as described above were loaded onto a discontinuous sucrose step gradient [45]. Briefly, the fraction was loaded into ultracentrifuge tubes between layers of sucrose buffers of increasing densities, in the following order: 2.5 ml 1.3 M sucrose, 3 ml 0.86 M sucrose, 4 ml supernatant from *A. fulica* whole body extraction, and 3 ml 0.25 M sucrose. The ultracentrifuge tubes containing the sucrose gradient and samples were carefully transported to the ultracentrifuge (100,000 ×*g*, 1 h, 4 °C, set with the brakes turned off and slowest possible acceleration). The SII interface (at 0.50/0.86 M) was collected using a wide bore transfer pipette. This fraction, enriched in stacked Golgi, was adjusted to 1.15 M sucrose using 2 M sucrose, layered at the bottom of the second step gradient and overlaid with equal volumes of 1.0, 0.86 and 0.25 M sucrose and centrifuged at 76,000 ×*g* for 3 h at 4 °C. The enriched Golgi fraction, located at the 0.25 M/0.86 M interface was collected, diluted with an equal volume of 0.1 M KH_2PO_4/K_2HPO_4 buffer, pH 6.7, pelleted for 60 min at 150,000 ×*g* and stored at −80 °C.

2.4. Stacked Golgi proteins extraction and analysis

The enriched Golgi fraction was delipidated by methanol/chloroform (4/1, v/v) extraction, and homogenised in a vortex. Double-distilled water (ddH_2O) was added to the mixture (3× the initial volume), vortexed and microcentrifuged (16,000 ×*g*, 2 min). The upper aqueous layer was removed, discarded and ddH_2O (3× vol) added to the

protein/chloroform mixture followed by vortexing. The proteins were then pelleted in a microcentrifuge at maximum speed for 2 min, suspended in 100 mM ammonium bicarbonate, pH 8.0, reduced with 5 mM DTT for 15 min at 50 °C, and the free thiol groups were alkylated with 10 mM iodoacetamide for 30 min at room temperature light protected and finally digested for 24 h at 37 °C with 1:100 ratio of 1 μg/μl mass spectrometry-grade trypsin (Thermo Scientific, Hayward, CA) [46]. Ten microliters of the digested Golgi fractions was analysed by multidimensional protein identification technology (MudPIT). Peptide mixtures were first separated by ion-exchange chromatography (Nucleosil®-SA SCX column, 5 μm, 0.3 ID × 150 mm, Macherey-Nagel Inc., Bethlehem, PA, USA) using seven steps of increasing ammonium chloride concentration (0, 50, 100, 150, 200, 300, and 600 mM). Each salt step was directly loaded onto the reversed phase column (Nucleosil-C18, 0.180 ID × 100 mm, Bethlehem, PA, USA) and separated with an acetonitrile gradient: eluent A, 0.1% formic acid in water; eluent B, 0.1% formic acid in acetonitrile. The samples were eluted (200 nl/min) in a gradient of 20–80% solvent B over 60 min (solvent A: 5% 2-propanol/0.2% formic acid; solvent B: 90% 2-propanol/0.2% formic acid) directly analysed in the nanospray source of a linear ion-trap mass spectrometer as described in Section 2.5.

2.5. Mass spectrometry

Tandem mass spectra were obtained on an LXQ linear ion-trap mass spectrometer (Finnigan, Thermo Fisher Scientific, Waltham, MA) at the Molecular Biology Program, Universidade Federal de São Paulo, Brazil. Proteoglycans were excised from the bands after SDS-PAGE separation, tryptic or proteinase K digested and submitted to LC/MS/MS analysis. LXQ settings were as follows: spray voltage of 1.8 kV, normal and zoom scan rates for full MS and MS/MS, respectively, 1 microscan for MS scans at a maximum inject time of 10 ms with a mass range of m/z 350–1400 and 3 microscans for MS/MS at a maximum inject time of 100 ms with automatic mass range. The isolation width was setup to 2.0 m/z and the activation Q parameter to 0.25, with activation time of 30 ms. A Dynamic Exclusion allowed one MS/MS scan per precursor ion followed by a 40 s exclusion period. The LXQ was operated in a data-dependent mode, that is, one MS scan for precursor ions followed by four data-dependent MS/MS scans for precursor ions above a threshold ion count of 500 with a normalised collision energy value of 35%. The MS/MS spectra obtained were used to search an UNIREF90 database (www.uniprot.org) using Sequest version 27.9 [47], and data processing and database searches were performed on Bioworks Browser 3.3.1 SP1 (Thermo Fisher Scientific). DTA files were generated from LC–MS/MS raw files with the following options: precursor ion tolerance of 1.5 amu, group scan 1, minimum group count 1, minimum ion count 20, and filtering through charge state analysis. The generated DTA files were searched against a composite target-decoy database [48] composed by a subset delimited with the strings sulphotransferase, epimerase and exostosis, for the search against the glycosaminoglycan modifying enzymes. No subset was used for proteoglycans database search. The database was concatenated with the reverse sequences of all the proteins in the database to allow for the determination of false-positive rates with the following criteria: enzyme, trypsin (KR/P) or proteinase K (depending of the enzyme used); full enzymatic cleavage; missed cleavage sites, 3; peptide tolerance, 2.0 amu; fragment ion tolerance, 1.0 amu; variable modifications, carbamidomethylation (+57 Da), methionine oxidation (+16 Da); modifications per peptide, 3. Those matches typically considered true matches had ΔCn scores of at least 0.1 and XCorr values of 2.0 or greater for +1 and +2 charged peptides, and 3.5 or greater for +3 charged peptides. For DTT modified peptides, a mass dynamic modification of 136.2 Da was set for serine and threonine residues. A mass increase of 120.2 Da was also allowed for a cysteine when we found that alkylated cysteines became derivatized using DTT. Major peptides with modifications were as follows: chondroitin sulphate (CSPG) (AEWDSS*GARG) and heparan sulphate proteoglycan (HSPG2) (YS*GRGD, S*GHCIPGDY). In cases in which more than one commonly occurring peptide was used for a particular proteoglycan, the signal intensities for the peptides were averaged. Stacked Golgi proteins were analysed as described previously [45].

2.6. Immunohistochemistry

Organs (mucous gland, oviduct, intestine, and eye) of five specimens of *A. fulica* were dissected and fixed in 4% buffered paraformaldehyde at 4 °C for 12 h, submerged in 30% sucrose for 24 h at 4 °C and embedded in tissue conditioning medium (Tissue Tek, Sakura Finetek Inc., Torrance, CA). Tissue sections (4 μm) were cut and washed in phosphate buffered saline (PBS) and unspecific protein binding sites blocked with 5% foetal bovine serum (FBS) in PBS for 30 min at 4 °C. The sections were then incubated with specific primary antibodies: goat anti-EXT1 (Santa Cruz sc-11040), goat anti-EXT2 (Santa Cruz sc-11045), mouse anti-NDST1 (Abgent AT2995a), mouse anti-NDST1 (Abgent AT2996a), mouse anti-epimerase (Abcam AB68714-50), rabbit anti-HS2ST1 (Abgent AP7648c), rabbit anti-HS2ST1 (Abgent AP2996a), rabbit anti-carbohydrate sulphotransferase 4-Golgi

Table 1
Identified proteoglycans from *A. fulica* extracts [a].

Protein name (Uniref accession numbers)	No of peptides	Predicted mass, kDa	Sequence coverage %
Versican (UPI0000EB4193, UPI000057FE02, UPI0000EB4193) TASSEEIHL, STAKATVPS[b], EPTTYVD, TVEGKEAFGP, PGTDAGMA	14	370,872	6
Perlecan (B1B0C7, UPI00006A1CD8, UPI00006A2F05, Q6KDZ1, UPI00015550) GFTVEP, APASPAPI, GSPIYLE, YYKGPT, HSSLITP[b], NHHIVK, PPLYYHW, GDRVHW[b], PLALLFF, HSSLITP[b], GKNVKP, HDSBEF[b], PGFYGDASAGT, YYKGPT	5	422,479	4
Aggrecan (UPI000069DE40, UPI0000F31294, Q95244) IVPATAAPAEA, QTEAPGTA[b], SSGITFVDT[b], EEPRIT	4	125,304	6
CSPG3 (P79787, Q1LVV8,Q5ISN4, UPI000184A15A) [c] AEWDSS*GARG, SVAPATPETT, PAMSTLASSSS, KILMEF	4	111,989	7
CSPG4-NG2 (UPI0001760E11, UPI00005A0919, Q6UVK1) PPATLKVV, QLLVGGR, LALGQKEL, PSPRPERSI[b], RGLEVN, TIEDALLL, MIQQPQGA	7	222,692	4
HSPG2 (UPI0001CBAD04, B2RZI0, UPI0000D9F8A3)[a] LPVDIGSSAKSVV, YS*GRGD, NPKTGDPQ, S*GHCIPGDY	4	371,316	3

[a] The complete list of all peptides identified for each proteoglycan is included in the supplemental material.
[b] Peptides from Proteinase K digests.
[c] Peptides with DTT tagging.

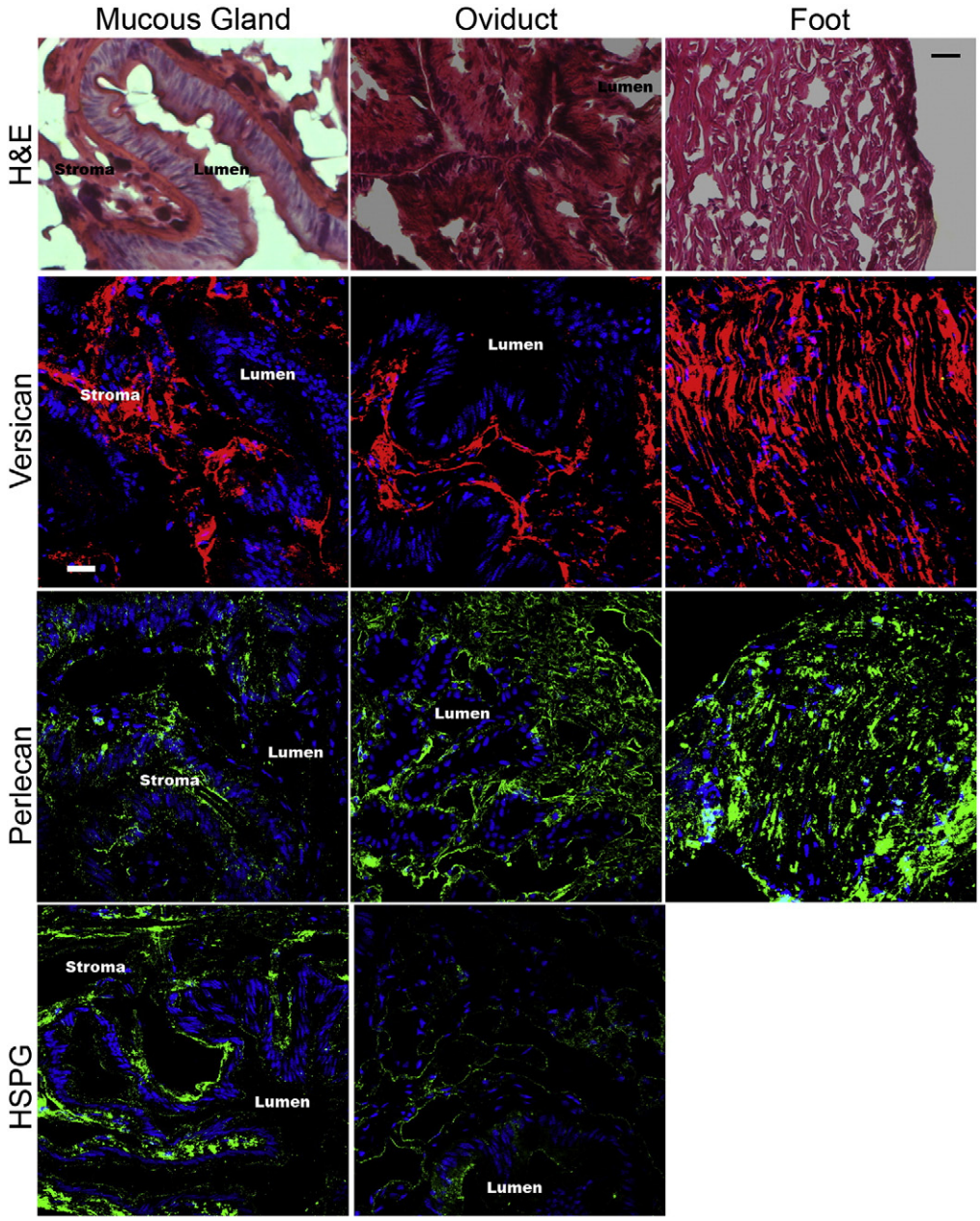

Fig. 1. Detection and localisation of versican, perlecan and heparan sulphate proteoglycan in tissues of *A. fulica* tissue sections. H&E staining and immunohistochemistry were performed on sections of the mucous gland oviduct and foot prepared from *A. fulica*. Different proteoglycans (versican, perlecan and HSPG) were detected through immunofluorescence and analysed using a Zeiss LSM510 scanning confocal inverted microscope. The nuclei (blue) were stained with DAPI. The white scale bar represents 20 μm. Images of H&E staining were obtained with an optical Nikon Eclipse E800 microscope. The blacks scale bar represents 20 μm.

marker (AB28742), goat anti-perlecan (Santa Cruz sc-27449), mouse anti-versican (Seikagaku), or mouse anti-HSPG (Seikagaku) for 16 h at 4 °C in blocking solution. Negative control was performed substituting the primary antibody with rabbit serum and did not yield specific immunostaining. Afterwards, the coverslips were washed three times in PBS and then incubated for 1 h at room temperature with appropriate fluorescent secondary antibodies produced in donkey conjugated to Alexa Fluor® 488 or Alexa Fluor® 594 (Molecular Probes/Invitrogen, Eugene, OR). The nuclei were stained with 4,6-diamidino-2-phenylindole (DAPI). After incubation with the antibodies, the coverslips were washed three times in PBS, mounted on glass slides in Fluoromount G (2:1 in PBS, Electron Microscopy Sciences, Hatfield, PA) and sealed with nail polish. Coverslips were examined using a Zeiss LSM510 scanning confocal inverted microscope and images analysed using LSM Image Browser 3.2 software (Zeiss, Germany).

3. Results

3.1. Proteoglycans typical of vertebrate tissues are present in A. fulica

Proteoglycans (PGs) such as versican, perlecan, and aggrecan were characterised for the first time in soft tissues of the mollusc *A. fulica* using a proteomic approach (Table 1, Supplementary Table 1 and Supplementary Fig. 1). From a total of 76 proteins and 271 peptides, twenty six proteoglycan core proteins were identified, with approximately 1.5% false discovery rate (FDR) at protein level. Perlecan and versican were identified with 6% (5 peptides) and 4% (14 peptides) protein sequence

Table 2
Glycosaminoglycan biosynthetic enzymes of *A. fulica* identified by Golgi proteomics.

Protein name (accession numbers)	No of peptides	Predicted mass, kDa	Sequence coverage %
Heparan sulphate 2-O-sulphotransferase (C4QHN0, D4I0001CBB25A, Q76KB1, Q86BJ3, Q8BUB6, UPI0000E48DC5, UPI0000EBD000, UPI0000ECC8D0, UPI00017588A1, UPI000180C6DA, UPI000186E22F, UPI0001CB95A9, UPI0001CBAA90, UPI0001CBBC67, UPI0001CBBEAC, UPI0001CBBEAE)	41	24,479	26
Heparan sulphate 3-O-sulphotransferase 1 (Q6YLY0, UPI0000ECAC02, Q8IZT8, UPI0001C613BF, Q9Y661, A7UFE0, O35310, Q96QJ5, UPI00003ADA1C, A0MGZ2)	23	34,841	32
Heparan sulphate 3-O-sulphotransferase 2 (UPI000180CE00, UPI0001CE1FE6, UPI000194C357, UPI00015B54E4, UPI0001CE1FE6, UPI0000F2C050, UPI0000F2D8AE, UPI000194D530, UPI00015B54E4, UPI0001C613BF, A0MGY7, UPI000069DCC7)	24	44,308	21
Heparan sulphate 3-O-sulphotransferase 3 (A7UFE0, UPI0001CE1137, UPI00005A4371)	6	32,896	9
Heparan sulphate 3-O-sulphotransferase 4 (A0MGZ0,UPI0000E46D7A,UPI0000F2DDA5,UPI0000D9E188,UPI0000EBDBAC, UPI0001CBB11F,UPI000180BB50,UPI0000DA1D7C)	16	48,227	16
N-deacetylase/N-sulphotransferase 1 (B0WMN5, C4Q3D0, C5BJN3, D2AWE5, Q3HKN9, Q9V3L1, UPI00003AD891, UPI000069EC32, UPI0000D9C374, UPI0000F2CA91, UPI00015B5745, UPI0001760624, UPI000180BCFF, UPI000194D19A)	34	113,157	23
N-deacetylase/N-sulphotransferase 2 (P52850, Q2S3V4, O95803)	5	101,202	4.2
N-deacetylase/N-sulphotransferase 3 (O95803)	2	100,902	3
6-O-sulphotransferase 1 (A8NI06, C4PY10, O6024, Q56UJ5, Q76KB2, Q8UWB1, Q96MM7, Q9QYK5, Q9VDR6, UPI0000587151, UPI00005A0E4B, UPI0000E4948D, UPI0000F2BBF4, UPI0000F2E085, UPI0000F2E110, UPI0000F2E643, UPI000155CF98, UPI000155E16F, UPI00017EFB83, UPI000194CCD1, UPI0001CB9B74, UPI0001CBBE9A, UPI0001CE1620)	53	48,910	31
CS/DS 6-O-sulphotransferase 2 (Q9VDR6)	2	52,676	2.4
CS/DS 4-O-sulphotransferase (B0W1J7, B0W401, B0WCF8, B1WBV7, B2GV63, B3DFJ6, B7QG53, Q08DS2, Q0D2D0, Q17NH2, Q28E26, UPI00006A5799, UPI0000D9454A, UPI0000F1D2AB, UPI00015B59E2, UPI0001797BBA, UPI000180BF19, UPI000194D354, UPI0001CE30CB)	46	43,075	45
CS/DS 3-O-sulphotransferase (B7PMT6, UPI00006A5E7A, UPI0000DA3209, UPI0000F2E32F, UPI0001CB9EAF, UPI0001CBA2ED, UPI0001CBA313, UPI0001CBB043, UPI0001CBB512, UPI0001CBB6BE, UPI0001CBBB07, UPI0001CBBDFD)	29	41,002	37
KS 6-O-sulphotransferase (UPI0000521A98, UPI00006A431D, UPI000180B495, UPI0001CBA1F2, UPI0001CBBA9A)	16	40,058	42
EXT 1 (UPI00006A127A)	1	74,050	4.2
EXT 2 (Q28F88, Q3TPI7, A0JN91, C9JU51, UPI000154D9B6, UPI00015DF52C)	32	74,527	21

coverage, respectively, with no putative GAG addition sites. Aggrecan showed 2 putative GAG attachment sites (AEWDSS*GARG and SSG*ITFVDT) with 6% sequence coverage in the 4 peptides found. Chondroitin sulphate proteoglycan-3 and -4 (Neuroglycan-NG2) were also found in the proteoglycan extracts with predicted molecular masses of 112 and 222 kDa and sequence coverage of 7 and 4%, respectively. Molluscs contain HS chains similar to those found in vertebrates [32]. Using the present methodology we were able to identify a heparan sulphate proteoglycan (HSPG2) with sequence coverage of 3% in 5 peptides found. Furthermore, putative attachment sites (YS*GRGD and S*GHCIPGDY) were identified for two of those peptides by DTT tagging.

3.2. Proteoglycans tissue distribution in A. fulica revealed by immunohistochemistry

Perlecan and versican were distributed throughout the integument of *A. fulica*. A similar pattern has been described for collagen type-I in other gastropods [49]. Our results showed that these PGs were localised in the extracellular matrix (ECM) of the subepidermal connective tissue. For perlecan, the distribution was occasionally thickened into clumps or irregularly branching forms with an intense meshwork of reactivity (Fig. 1). The reactivity for both versican and perlecan was particularly strong in the mucous gland, oviduct, and foot. HSPG was detected in all organs analysed; however, the distribution of this proteoglycan was strong and organised in the mucous gland and oviduct, with substantial immunoreactivity in the acinar epithelial cells, as well as, a lamellar distribution throughout the organs. HSPG was also strongly detected in the stroma surrounding the acinar glands and this distribution was thickened into clumps. The distribution of HSPG suggests a role in the support of the acinar epithelial cells, possibly forming a basal membrane surrounding this structure. In the oviduct, mucous gland and foot the versican antibody staining showed intense meshwork of positive staining with strong immunoreactivity in the foot between bundles of muscle fibres (Fig. 1).

3.3. Enzymes involved in GAG biosynthesis discovered by peptide analysis of A. fulica Golgi extracts

An initial assessment of GAG biosynthetic machinery in the whole body of *A. fulica* was performed on enriched Golgi fractions and analysed by multidimensional protein identification technology (MudPIT) LC–MS/MS. From 1032 total peptide sequences found, we found 384 peptides from *A. fulica* which were matched to 118 GAG biosynthetic proteins (Table 2 and Supporting information Table 2). With the exception of glucuronosyl C5-epimerase, peptides were found for all enzymes responsible for heparan sulphate/heparin biosynthesis. Enzymes putatively related to chondroitin sulphate (CS) and dermatan sulphate (DS) synthesis were also detected.

3.4. Glycosaminoglycan biosynthetic enzymes in A. fulica tissues revealed by immunohistochemistry

Glycosaminoglycan biosynthetic enzymes showed remarkable distribution in the oviduct and mucous gland tissues, surrounding acinar and bundles of muscle fibre, being particularly numerous in the gastropod integument (Fig. 2). The staining of heparan sulphate 2-O-

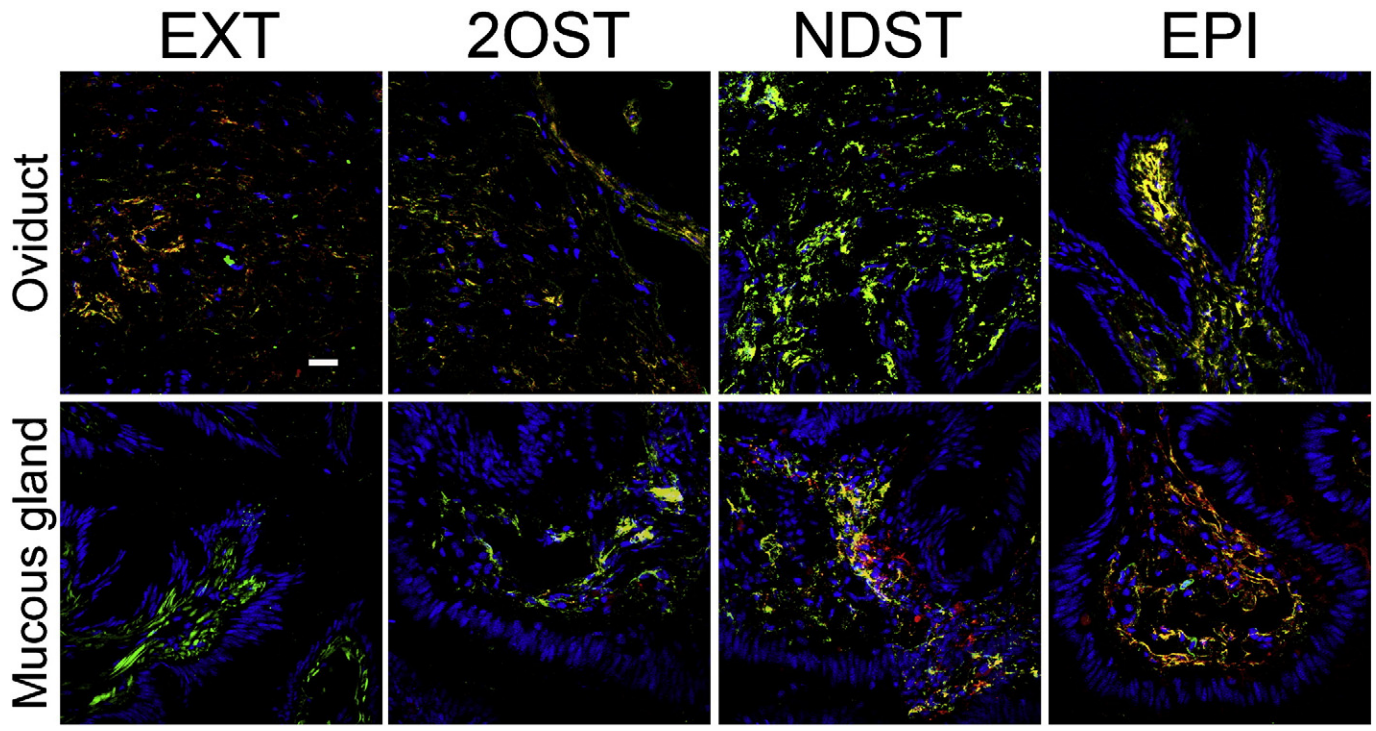

Fig. 2. Detection and localisation of enzymes involved in heparan sulphate biosynthesis in *A. fulica* tissue sections. Immunohistochemistry analysis was performed on mucous gland and oviduct tissue sections prepared from *A. fulica* and different enzymes involved in heparan sulphate biosynthesis investigated by immunohistochemistry. EXT1 (heparan sulphate polymerase 1), EXT2 (heparan sulphate polymerase 2), 2OST (heparan sulphate 2-O-sulphotransferase), NDST1 (heparan sulphate N-deacetylase/N-sulphotransferase 1) and Epi (glucuronosyl C5-epimerase) were detected with Alexa 488 (green) and Carbohydrate sulphotransferase-4 (Golgi marker) detected with Alexa 594 (red) with exception to EXT1 in the mucous gland. Co-localisation of channels is represented in yellow. Immunofluorescence was detected using a Zeiss LSM510 scanning confocal inverted microscope. The nuclei (blue) were stained with DAPI. Scale bar represents 20 μm.

sulphotransferase was strong adjacent to the epithelium and discontinuous in the connective tissue. Glucuronosyl C5-epimerase antibody staining was present in the zone between the epithelium and the underlying connective tissue but occasionally concentrated into irregular clumps (Fig. 2 and Supplementary Fig. 2). Similar staining profile was observed for the heparan sulphate polymerases (EXT1 and EXT2). The NDST antibody staining was discontinuous and irregular (Fig. 2 and Supplementary Fig. 2). All GAG biosynthetic enzymes investigated herein colocalised with carbohydrate sulphotransferase 4, which is a Golgi marker, thus confirming the Golgi localisation for these enzymes.

4. Discussion

The diversity in structure and specific cellular and tissue distribution indicates that these glycoconjugates could perform different biological roles. Indeed, pivotal functions have been postulated for proteoglycans and their GAG moieties, such as organisation and modulation of the extracellular matrix, tissue morphogenesis and differentiation, cellular adhesion and recognition, amongst others [26,50]. Nevertheless, the information on the distribution and characterisation of proteoglycans in invertebrate tissues is limited and restricted to a few species [50–56]. Our data shows for the first time the presence and tissue localisation of different proteoglycans in organs of the gastropoda *A. fulica*. Furthermore, these proteoglycans show tissue distribution and structural characteristics similar to those found in vertebrate species. Thus, the presence of versican, a CS proteoglycan classically of the ECM, was detected in the snail tissues through immunohistochemistry, showing the same type of arrangement first described for collagens in other molluscs [57]. Perlecan, another CS or HS proteoglycan from ECM was also clearly demonstrated in the tissues analysed, presenting a similar distribution. Furthermore, the core proteins for these PGs were confirmed by proteomic analysis. The presence of HSPG, a classic cell membrane proteoglycan, was identified through immunohistochemistry at the cell surface as described for vertebrate species. Furthermore, other ECM PGs, such as aggrecan (CSPG-1) and neurocan (CSPG-3), and neuroglycan (CSPG4-NG2), a transmembrane PG, were detected solely through proteomic analysis. These combined data are indicative of the strong relationship between invertebrate and vertebrate proteoglycans, thereby suggesting a common pattern of biological activity in invertebrates.

Regarding the enzymes involved in GAG biosynthesis, our results clearly demonstrated both by the peptide profiling from Golgi proteins as well as tissue localisation by immunohistochemistry that the snail has the complete biosynthetic machinery necessary to synthesise HS, HEP, as well as AS. We were able to show the enzymes involved in the initial steps of polymer formations (polymerases I and II, EXT 1 and EXT 2) as well as the ones related to secondary modifications, such as N-deacetylation/N-sulphation of the glucosamine moiety, epimerization of the β-D-glucuronic acid to α-L-iduronic acid, and O-sulphation at various positions of the polymer chain, that is, at the uronic acid and the glucosamine moieties (2OST, 3OST, 6OST). Regarding the biosynthetic machinery for CS, using the proteomic analysis we showed the presence of different sulphotransferases. Therefore, our novel technique of Golgi proteomics of *A. fulica* revealed the presence of conserved GAG biosynthetic machinery [16,58–64].

5. Conclusion

Limiting factors of proteomic approaches include the subsequent characterisation of the identified proteins and the amount of false positive results due to the lack of a robust data analysis and validation. This can be even greater when one studies molecules from a new model, where most of the data need further validation. In contrast, our present study not only identifies GAG biosynthetic enzymes through proteomic analysis of stacked Golgi isolation and provides further

information on the machinery involved, but also provides a novel method for the study related to GAG and proteoglycan evolution.

Supplementary materials related to this article can be found online at doi:10.1016/j.bbapap.2011.07.024.

Acknowledgements

We are grateful to Claudia Blanes Angeli for helping with column packing and Prof. Dr. Carlos Bloch Jr. for his critical view of the results. This work was supported by Fundação de Amparo à Pesquisa do Estado de São Paulo (FAPESP), Conselho Nacional do Desenvolvimento Científico e Tecnológico (CNPq) and Coordenação de Aperfeiçoamento de Pessoal de Nível Superior (CAPES). ICA is supported by NIH grants 2G12RR008124-16A1 and 2G12RR008124-16A1S1.

References

[1] M.A. Bourdon, T. Krusius, S. Campbell, N.B. Schwartz, E. Ruoslahti, Identification and synthesis of a recognition signal for the attachment of glycosaminoglycans to proteins, Proc. Natl. Acad. Sci. U. S. A. 84 (1987) 3194–3198.
[2] C.P. Dietrich, J.F. de Paiva, C.T. Moraes, H.K. Takahashi, M.A. Porcionatto, H.B. Nader, Isolation and characterization of a heparin with high anticoagulant activity from *Anomalocardia brasiliana*, Biochim. Biophys. Acta 843 (1985) 1–7.
[3] C.P. Dietrich, H.B. Nader, V. Buonassisi, P. Colburn, Inhibition of synthesis of heparan sulfate by selenate: possible dependence on sulfation for chain polymerization, FASEB J. 2 (1988) 56–59.
[4] C.P. Dietrich, H.B. Nader, J.F. de Paiva, E.A. Santos, K.R. Holme, A.S. Perlin, Heparin in molluscs: chemical, enzymatic degradation and 13C and 1H n.m.r. spectroscopical evidence for the maintenance of the structure through evolution, Int. J. Biol. Macromol. 11 (1989) 361–366.
[5] L. Toma, M.A. Pinhal, C.P. Dietrich, H.B. Nader, C.B. Hirschberg, Transport of UDP-galactose into the Golgi lumen regulates the biosynthesis of proteoglycans, J. Biol. Chem. 271 (1996) 3897–3901.
[6] J.D. Esko, L. Zhang, Influence of core protein sequence on glycosaminoglycan assembly, Curr. Opin. Struct. Biol. 6 (1996) 663–670.
[7] B. Kuberan, M. Ethirajan, X.V. Victor, V. Tran, K. Nguyen, A. Do, "Click" xylosides initiate glycosaminoglycan biosynthesis in a mammalian cell line, ChemBioChem 9 (2008) 198–200.
[8] L.S. Lohmander, T. Shinomura, V.C. Hascall, J.H. Kimura, Xylosyl transfer to the core protein precursor of the rat chondrosarcoma proteoglycan, J. Biol. Chem. 264 (1989) 18775–18780.
[9] B.M. Vertel, L.M. Walters, N. Flay, A.E. Kearns, N.B. Schwartz, Xylosylation is an endoplasmic reticulum to Golgi event, J. Biol. Chem. 268 (1993) 11105–11112.
[10] J. Angulo, R. Ojeda, J.L. de Paz, R. Lucas, P.M. Nieto, R.M. Lozano, M. Redondo-Horcajo, G. Gimenez-Gallego, M. Martin-Lomas, The activation of fibroblast growth factors (FGFs) by glycosaminoglycans: influence of the sulfation pattern on the biological activity of FGF-1, ChemBioChem 5 (2004) 55–61.
[11] J.R. Couchman, Transmembrane signaling proteoglycans, Annu. Rev. Cell Dev. Biol. 26 (2010) 89–114.
[12] J.L. Dreyfuss, C.V. Regatieri, M.A. Lima, E.J. Paredes-Gamero, A.S. Brito, S.F. Chavante, R. Belfort Jr., M.E. Farah, H.B. Nader, A heparin mimetic isolated from a marine shrimp suppresses neovascularization, J. Thromb. Haemost. 8 (2010) 1828–1837.
[13] Y.S. Lee, H.O. Yang, K.H. Shin, H.S. Choi, S.H. Jung, Y.M. Kim, D.K. Oh, R.J. Linhardt, Y.S. Kim, Suppression of tumor growth by a new glycosaminoglycan isolated from the African giant snail *Achatina fulica*, Eur. J. Pharmacol. 465 (2003) 191–198.
[14] D.W. Li, I.S. Lee, J.S. Sim, T. Toida, R.J. Linhardt, Y.S. Kim, Long duration of anticoagulant activity and protective effects of acharan sulfate in vivo, Thromb. Res. 113 (2004) 67–73.
[15] C.M. Cassaro, C.P. Dietrich, Distribution of sulfated mucopolysaccharides in invertebrates, J. Biol. Chem. 252 (1977) 2254–2261.
[16] B. Kuberan, M. Lech, J. Borjigin, R.D. Rosenberg, Light-induced 3-O-sulfotransferase expression alters pineal heparan sulfate fine structure. A surprising link to circadian rhythm, J. Biol. Chem. 279 (2004) 5053–5054.
[17] G.F. Medeiros, A. Mendes, R.A. Castro, E.C. Bau, H.B. Nader, C.P. Dietrich, Distribution of sulfated glycosaminoglycans in the animal kingdom: widespread occurrence of heparin-like compounds in invertebrates, Biochim. Biophys. Acta 1475 (2000) 287–294.
[18] G. Sugumaran, M. Katsman, J.E. Silbert, Subcellular co-localization and potential interaction of glucuronosyltransferases with nascent proteochondroitin sulphate at Golgi sites of chondroitin synthesis, Biochem. J. 329 (Pt 1) (1998) 203–208.
[19] D.H. Kim, B.T. Kim, S.Y. Park, N.Y. Kim, M.J. Han, K.H. Shin, W.S. Kim, Y.S. Kim, Degradation of acharan sulfate and heparin by Bacteroides stercoris HJ-15, a human intestinal bacterium, Arch. Pharm. Res. 21 (1998) 576–580.
[20] Y.S. Kim, M.Y. Ahn, S.J. Wu, D.H. Kim, T. Toida, L.M. Teesch, Y. Park, G. Yu, J. Lin, R.J. Linhardt, Determination of the structure of oligosaccharides prepared from acharan sulfate, Glycobiology 8 (1998) 869–877.
[21] Y.S. Kim, Y.Y. Jo, I.M. Chang, T. Toida, Y. Park, R.J. Linhardt, A new glycosaminoglycan from the giant African snail *Achatina fulica*, J. Biol. Chem. 271 (1996) 11750–11755.
[22] J. Presto, M. Thuveson, P. Carlsson, M. Busse, M. Wilen, I. Eriksson, M. Kusche-Gullberg, L. Kjellen, Heparan sulfate biosynthesis enzymes EXT1 and EXT2 affect NDST1 expression and heparan sulfate sulfation, Proc. Natl. Acad. Sci. U. S. A. 105 (2008) 4751–4756.
[23] X.V. Victor, T.K. Nguyen, M. Ethirajan, V.M. Tran, K.V. Nguyen, B. Kuberan, Investigating the elusive mechanism of glycosaminoglycan biosynthesis, J. Biol. Chem. 284 (2009) 25842–25853.
[24] T.M. Ferreira, M.G. Medeiros, C.P. Dietrich, H.B. Nader, Structure of heparan sulfate from the fresh water mollusc Anomantidae sp: sequencing of its disaccharide units, Int. J. Biochem. 25 (1993) 1219–1225.
[25] M. Gutternigg, K. Ahrer, H. Grabher-Meier, S. Burgmayr, E. Staudacher, Neutral N-glycans of the gastropod *Arion lusitanicus*, Eur. J. Biochem. 271 (2004) 1348–1356.
[26] K.H. Khoo, D. Chatterjee, J.P. Caulfield, H.R. Morris, A. Dell, Structural mapping of the glycans from the egg glycoproteins of *Schistosoma mansoni* and *Schistosoma japonicum*: identification of novel core structures and terminal sequences, Glycobiology 7 (1997) 663–677.
[27] H.B. Nader, T.M. Ferreira, J.F. Paiva, M.G. Medeiros, S.M. Jeronimo, V.M. Paiva, C.P. Dietrich, Isolation and structural studies of heparan sulfates and chondroitin sulfates from three species of molluscs, J. Biol. Chem. 259 (1984) 1431–1435.
[28] K. Sandra, P. Dolashka-Angelova, B. Devreese, J. Van Beeumen, New insights in *Rapana venosa* hemocyanin N-glycosylation resulting from on-line mass spectrometric analyses, Glycobiology 17 (2007) 141–156.
[29] O. Habuchi, K. Sugiura, N. Kawai, Glucose branches in chondroitin sulfates from squid cartilage, J. Biol. Chem. 252 (1977) 4570–4576.
[30] J. Jeong, T. Toida, Y. Muneta, I. Kosiishi, T. Imanari, R.J. Linhardt, H.S. Choi, S.J. Wu, Y.S. Kim, Localization and characterization of acharan sulfate in the body of the giant African snail *Achatina fulica*, Comp. Biochem. Physiol. B: Biochem. Mol. Biol. 130 (2001) 513–519.
[31] A.K. Ghosh, N. Hirasawa, Y.S. Lee, Y.S. Kim, K.H. Shin, N. Ryu, K. Ohuchi, Inhibition by acharan sulphate of angiogenesis in experimental inflammation models, Br. J. Pharmacol. 137 (2002) 441–448.
[32] E.J. Joo, G.B. ten Dam, T.H. van Kuppevelt, T. Toida, R.J. Linhardt, Y.S. Kim, Nucleolin: acharan sulfate-binding protein on the surface of cancer cells, Glycobiology 15 (2005) 1–9.
[33] Y. Park, Z. Zhang, T.N. Laremore, B. Li, J.S. Sim, A.R. Im, M.Y. Ahn, Y.S. Kim, R.J. Linhardt, Variation of acharan sulfate and monosaccharide composition and analysis of neutral N-glycans in African giant snail (*Achatina fulica*), Glycoconj. J. 25 (2008) 863–877.
[34] P. Talusan, S. Bedri, S. Yang, T. Kattapuram, N. Silva, P.J. Roughley, J.R. Stone, Analysis of intimal proteoglycans in atherosclerosis-prone and atherosclerosis-resistant human arteries by mass spectrometry, Mol. Cell Proteomics 4 (2005) 1350–1357.
[35] H. Blum, H. Beier, H.J. Gross, Improved silver staining of plant proteins, RNA and DNA in polyacrylamide gels, Electrophoresis 8 (1987) 93–99.
[36] A. Shevchenko, M. Wilm, O. Vorm, M. Mann, Mass spectrometric sequencing of proteins silver-stained polyacrylamide gels, Anal. Chem. 68 (1996) 850–858.
[37] C.C. Wu, J.R. Yates III, The application of mass spectrometry to membrane proteomics, Nat. Biotechnol. 21 (2003) 262–267.
[38] C.L. Gatlin, G.R. Kleemann, L.G. Hays, A.J. Link, J.R. Yates III, Protein identification at the low femtomole level from silver-stained gels using a new fritless electrospray interface for liquid chromatography-microspray and nanospray mass spectrometry, Anal. Biochem. 263 (1998) 93–101.
[39] L. Wells, K. Vosseller, R.N. Cole, J.M. Cronshaw, M.J. Matunis, G.W. Hart, Mapping sites of O-GlcNAc modification using affinity tags for serine and threonine post-translational modifications, Mol. Cell Proteomics 1 (2002) 791–804.
[40] D.P.a.J. Rossier, Organelle Proteomics, 2008.
[41] J.R. Stone, J.L. Maki, T. Collins, Basal and hydrogen peroxide stimulated sites of phosphorylation in heterogeneous nuclear ribonucleoprotein C1/C2, Biochemistry 42 (2003) 1301–1308.
[42] J. Eng, A. McCormack, J. Yates, An approach to correlate tandem mass spectral data of peptides with amino acid sequences in a protein database, J. Am. Soc. Mass Spectrom. 5 (1994) 976–989.
[43] J.L. Arias, A. Neira-Carrillo, J.I. Arias, C. Escobar, M. Bodero, M. David, M.S. Fernandez, Sulfated polymers in biological mineralization: a plausible source for bio-inspired engineering, J. Mater. Chem. 14 (2004) 2154–2160.
[44] T. Lecuit, Current topics in developmental biology tissue remodeling and epithelial morphogenesis preface, Tissue Remodeling Epithelial Morphog. 89 (2009) 15–42.
[45] C.Z. Li, Y.L. Hu, J. Liang, Y.W. Kong, J. Huang, Q.L. Feng, S.O. Li, G.Y. Zhang, L.P. Xie, R.Q. Zhang, Calcineurin plays an important role in the shell formation of pearl oyster (*Pinctada fucata*), Mar. Biotechnol. 12 (2010) 100–110.
[46] K.B. Lee, J.S. Kim, S.T. Kwak, W. Sim, J.H. Kwak, Y.S. Kim, Isolation and identification of chondroitin sulfates from the mud snail, Arch. Pharmacal Res. 21 (1998) 555–558.
[47] N. Volpi, F. Maccari, Purification and characterization of hyaluronic acid from the mollusc bivalve *Mytilus galloprovincialis*, Biochimie 85 (2003) 619–625.
[48] S. Faller, S. Staubach, A. Klussmann-Kolb, Comparative immunohistochemistry of the cephalic sensory organs in Opisthobranchia Mollusca, Gastropoda, Zoomorphology 127 (2008) 227–239.
[49] B.V. Nusgens, Hyaluronic acid and extracellular matrix: a primitive molecule? Ann. Dermatol. Venereol. 137 (Suppl. 1) (2010) S3–S8.
[50] S. Mizuguchi, T. Uyama, H. Kitagawa, K.H. Nomura, K. Dejima, K. Gengyo-Ando, S. Mitani, K. Sugahara, K. Nomura, Chondroitin proteoglycans are involved in cell division of *Caenorhabditis elegans*, Nature 423 (2003) 443–448.
[51] G. Pejler, A. Danielsson, I. Bjork, U. Lindahl, H.B. Nader, C.P. Dietrich, Structure and antithrombin-binding properties of heparin isolated from the clams *Anomalocardia brasiliana* and *Tivela mactroides*, J. Biol. Chem. 262 (1987) 11413–11421.
[52] L.O. Sampaio, H.B. Nader, Emergence and structural characteristics of chondroitin sulfates in the animal kingdom, Adv. Pharmacol. 53 (2006) 233–251.

[53] M. Tsuda, K. Kamimura, H. Nakato, M. Archer, W. Staatz, B. Fox, M. Humphrey, S. Olson, T. Futch, V. Kaluza, E. Siegfried, L. Stam, S.B. Selleck, The cell-surface proteoglycan Dally regulates Wingless signalling in Drosophila, Nature 400 (1999) 276–280.
[54] P. Hovingh, A. Linker, Glycosaminoglycans in two mollusks, *Aplysia californica* and *Helix aspersa*, and in the leech, *Nephelopsis obscura*, Comp. Biochem. Physiol. B: Biochem. Mol. Biol. 119 (1998) 691–696.
[55] J. Huxley-Jones, D.L. Robertson, R.P. Boot-Handford, On the origins of the extracellular matrix in vertebrates, Matrix Biol. 26 (2007) 2–11.
[56] S.K. Olson, J.R. Bishop, J.R. Yates, K. Oegema, J.D. Esko, Identification of novel chondroitin proteoglycans in *Caenorhabditis elegans*: embryonic cell division depends on CPG-1 and CPG-2, J. Cell Biol. 173 (2006) 985–994.
[57] A. Tetsukawa, J. Nakamura, S. Fujiwara, Identification of chondroitin/dermatan sulfotransferases in the protochordate, *Ciona intestinalis*, Comp. Biochem. Physiol. B: Biochem. Mol. Biol. 157 (2010) 205–212.
[58] L.K. Yeh, C.Y. Liu, W.W. Kao, C.J. Huang, F.R. Hu, C.L. Chien, I.J. Wang, Knockdown of zebrafish lumican gene (zlum) causes scleral thinning and increased size of scleral coats, J. Biol. Chem. 285 (2010) 28141–28155.
[59] J.J. Zoeller, W. Pimtong, H. Corby, S. Goldoni, A.E. Iozzo, R.T. Owens, S.Y. Ho, R.V. Iozzo, A central role for decorin during vertebrate convergent extension, J. Biol. Chem. 284 (2009) 11728–11737.
[60] S. Corbetta, A. Bairati, L. Vitellaro Zuccarello, Immunohistochemical study of subepidermal connective of molluscan integument, Eur. J. Histochem. 46 (2002) 259–272.
[61] N.K. Karamanos, A. Manouras, T. Tsegenidis, C.A. Antonopoulos, Isolation and chemical study of the glycosaminoglycans from squid cornea, Int. J. Biochem. 23 (1991) 67–72.
[62] H.B. Nader, M.G.L. Medeiros, J.F. Paiva, V.M.P. Paiva, S.M.B. Jeronimo, F. T.M.P.C, C.P. Dietrich, A correlation between the sulfated glycosaminoglycan concentration and degree of salinity of the habitat in fifteen species of the classes crustacea, pelecypoda and gastropoda, Comp. Biochem. Physiol. A: Mol. Integr. Physiol. 76 (1983) 433–436.
[63] R.P. Vieira, B. Mulloy, P.A. Mourao, Structure of a fucose-branched chondroitin sulfate from sea cucumber. Evidence for the presence of 3-O-sulfo-beta-D-glucuronosyl residues, J. Biol. Chem. 266 (1991) 13530–13536.
[64] R. Lawrence, S.K. Olson, R.E. Steele, L. Wang, R. Warrior, R.D. Cummings, J.D. Esko, Evolutionary differences in glycosaminoglycan fine structure detected by quantitative glycan reductive isotope labeling, J. Biol. Chem. 283 (2008) 33674–33684.
[65] T.F. Gesteira, V.J. Coulson-Thomas, A. Taunay-Rodrigues, V. Oliveira, B.E. Thacker, M.A. Juliano, R. Pasqualini, W. Arap, I.L. Tersariol, H.B. Nader, et al., Inhibitory peptides of the sulfotransferase domain of the heparan sulfate enzyme, N-deacetylase-N-sulfotransferase-1, J. Biol. Chem. 286 (2011) 5338–5346.